

# THE LANCET

## Supplementary appendix

This appendix formed part of the original submission and has been peer reviewed.  
We post it as supplied by the authors.

Supplement to: Gnechi M, Moretti F, Bassi EM, et al. Myocarditis in a 16-year-old boy positive for SARS-CoV-2. *Lancet* 2020; **395**: e116.

## **Supplementary appendix**

## Supporting figures

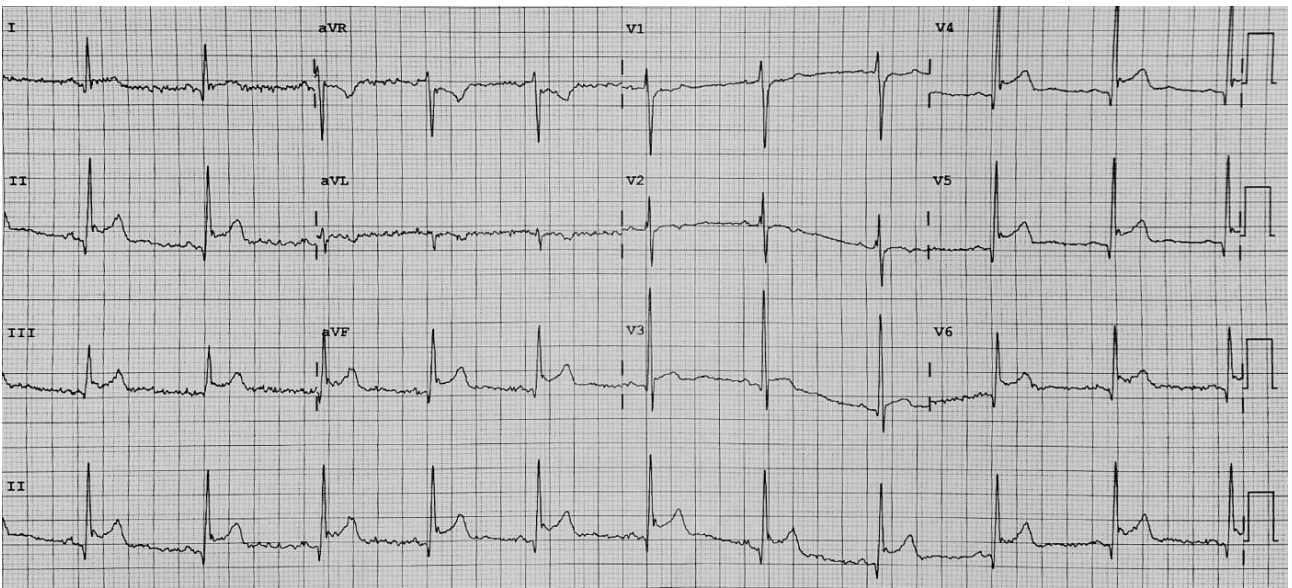


**Figure S1.** Control electrocardiogram recorded during the chest pain episode occurred the first night of hospitalization (hospital day one, 10:15 pm). No significant differences were present compared with the previous trace.

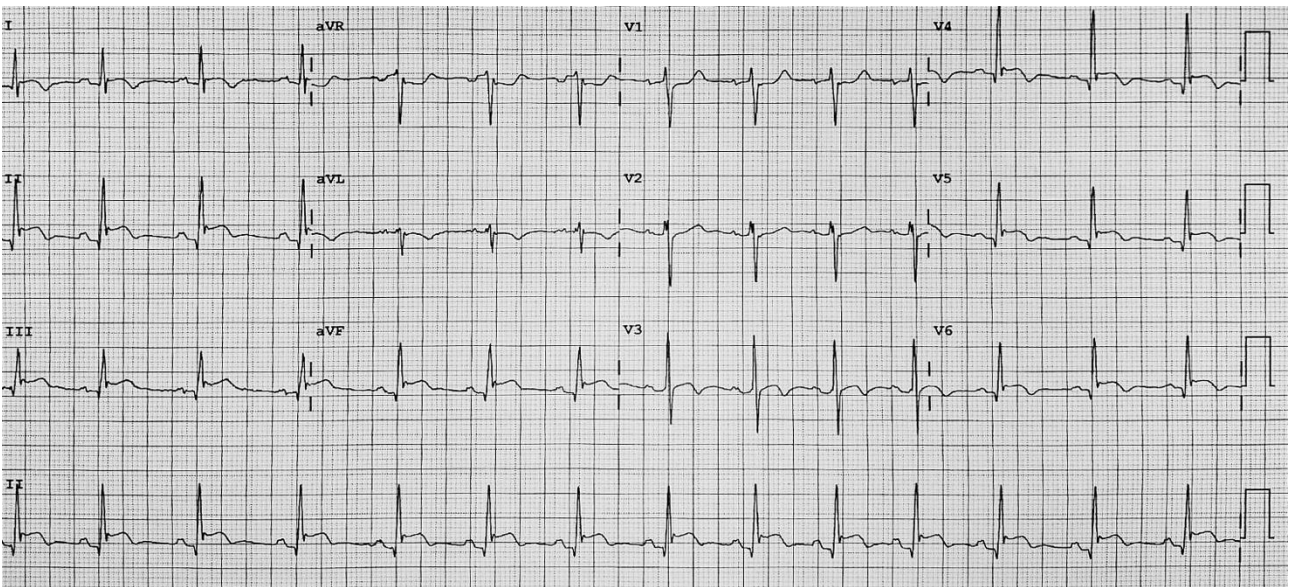


**Figure S2.** Control electrocardiogram (hospital day 2, 1:09 pm). Partial resolution of the ST-segment elevation in all leads, negative T waves in the lateral leads (I, aVL) and diphasic T waves in V3.

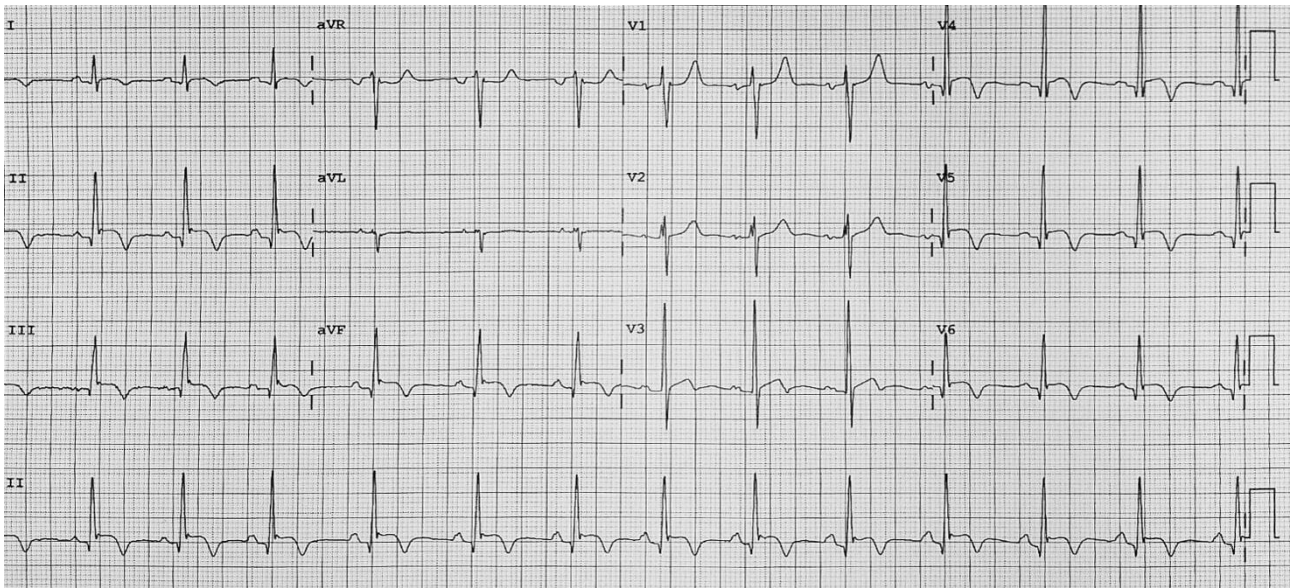


**Figure S3.** Control electrocardiogram (hospital day 3, 10:42 am). Evolution in the infero-lateral leads with appearance of negative T waves.

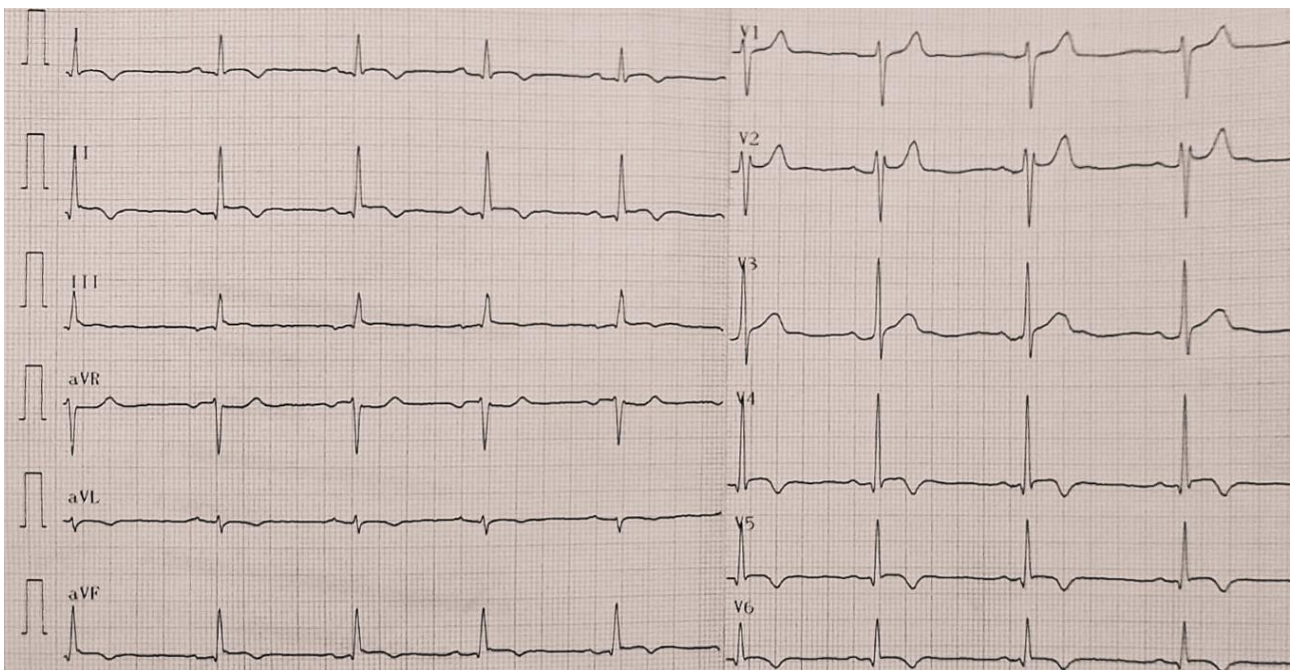


**Figure S4.** Control electrocardiogram recorded before transferring the patient to the COVID-19 Unit (hospital day 4). Further reduction of the residual ST-segment elevation with persistence of negative T waves in infero-lateral leads. Appearance of the rSr' pattern in V2 consistent with right ventricular activation delay.

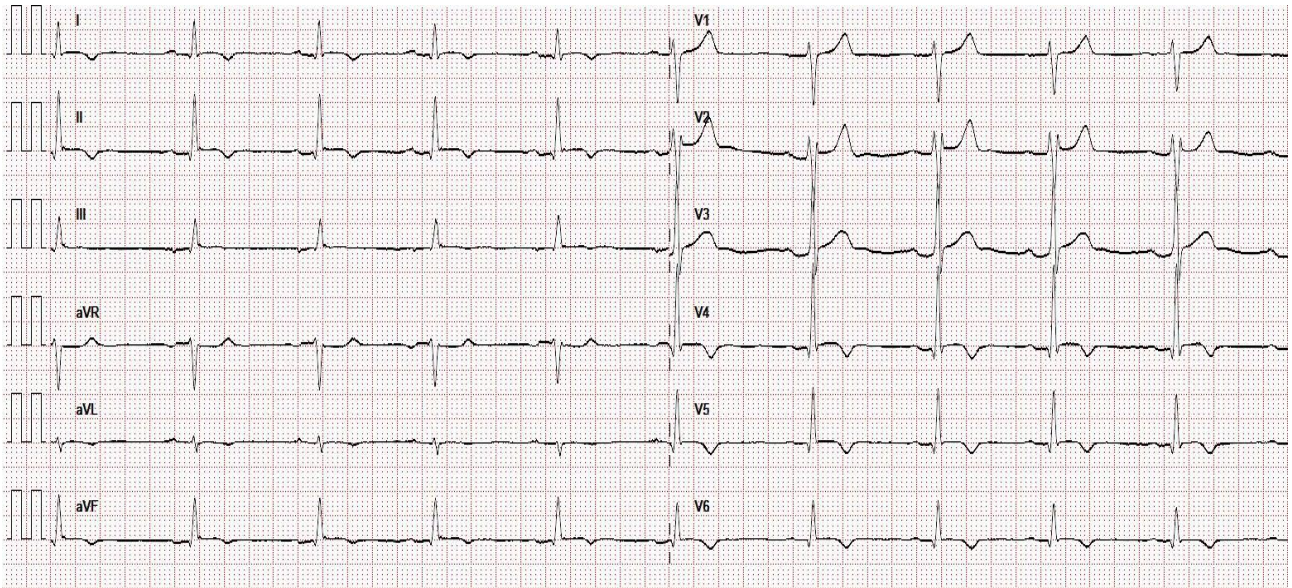


**Figure S5.** Hospital discharge electrocardiogram (hospital day 12, 11:31 am). Resolution of the ST-segment elevation with persistence of both negative T waves in the infero-lateral leads and rSr' pattern.



**Figure S6.** Posteroanterior Chest X-Ray. No pleural or pulmonary abnormalities were found.

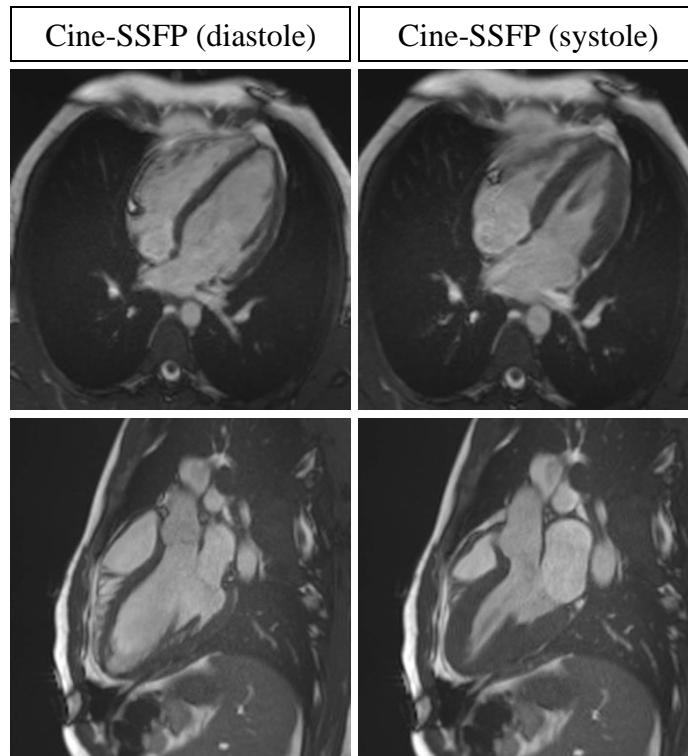


**Figure S7.** Cine-steady-state free precession images of four and three chambers long-axis view in end-diastolic and end-systolic phase show normal volumes and wall thickness and preserved biventricular systolic function.

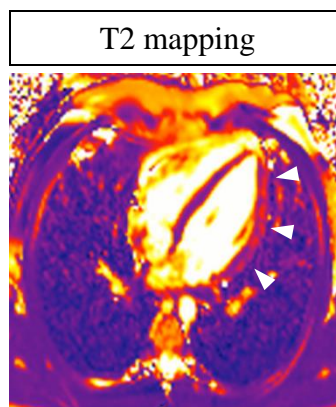


**Figure S8.** Cardiac magnetic resonance T2 mapping sequences demonstrating the presence of patchy oedema of the lateral wall.

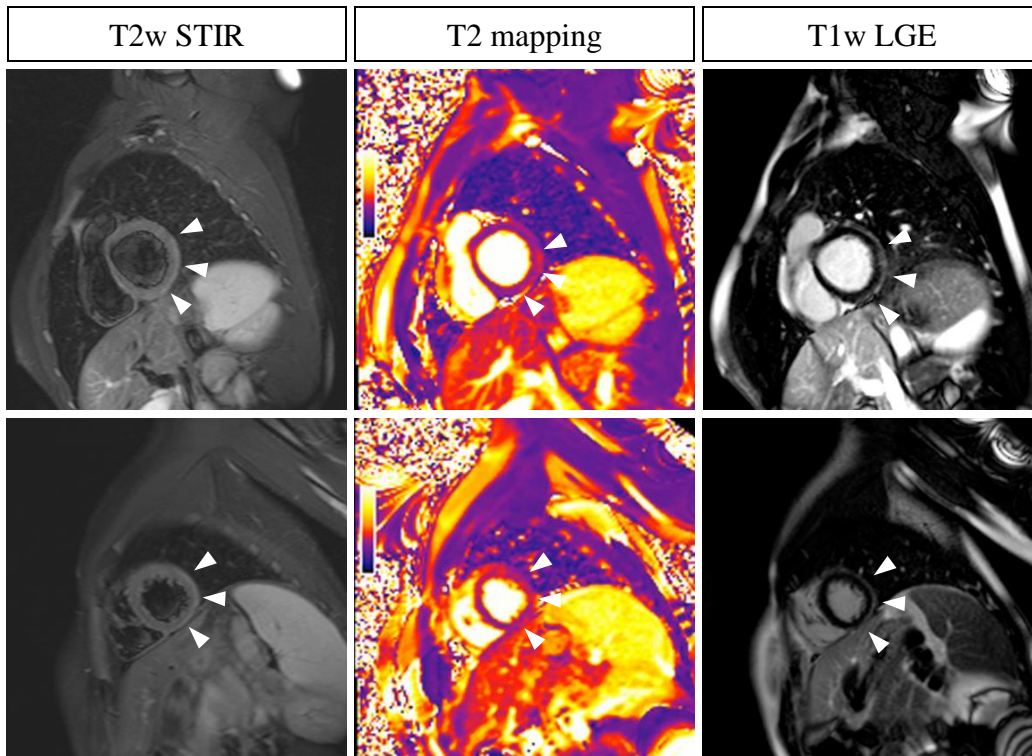


**Figure S9.** Cardiac magnetic resonance images of short axis projection of the basal (top panels) and mid segments are reported. T2w-STIR images show subepicardial band-like high signal demonstrating the presence of oedema at the level of inferior and infero-lateral walls, and patchy oedema pattern involving the whole lateral wall. T2 mapping sequences confirm the presence of oedema in the same segments. Finally, the late gadolinium sequences reveal high intensity signal indicating necrosis with the same distribution and localization.

## Supporting tables

<b>Table S1. Clinical laboratory results</b>									
<b>Measure</b>	<b>Reference range</b>	<b>Day 1</b>	<b>Day 2</b>	<b>Day 3</b>	<b>Day 4</b>	<b>Day 5</b>	<b>Day 6</b>	<b>Day 7</b>	<b>Day 8</b>
Alanine aminotransferase (mU/mL)	11.0 – 34.0	23.0	32.0	..	..	19.0	18.0	..	24.0
Amylase (mU/mL)	25.0 – 125.0	71.0	58.0	..	..	67.0	73.0	..	74.0
Total Bilirubinaemia (mg/dL)	0.2 – 1.1	1.33	1.17	1.12	..	1.49	3.18	..	2.48
Direct Bilirubinaemia (mg/dL)	0.00 – 0.25	0.49	..	..	..	0.53	0.96	..	0.77
Sodium (mEq/L)	135 – 153	136	139	..	..	139	140	139	137
Potassium (mEq/L)	3.50 – 5.30	3.55	4.45	..	..	3.70	4.04	3.94	4.09
Chloride (mEq/L)	94.0 – 110.0	100.0	104.0	..	..	105.0	104.0	..	100.0
Calcium (mg/dL)	8.60 – 10.30	9.10	8.80	..	..	9.10	9.20	..	9.30
Creatinine (mg/dL)	0.73 – 1.18	0.87	0.84	..	..	0.89	0.96	1.02	1.11
Urea (mg/dL)	10.0 – 50.0	32.0	30.0	..	..	42.0	44.0	43.0	50.0
Glucose (mg/dL)	76.0 – 110.0	106.0	91.0	..	..	124.0	80.0	..	71.0
Lactate dehydrogenase (mU/mL)	125.0 – 220.0	276.0	..	281.0	275.0	246.0	248.0	253.0	229.0
C-reactive protein (mg/dL)	<0.5	3.25	6.20	3.33	1.67	0.95	..	0.40	0.29
Procalcitonin (ng/mL)	0.00 – 0.50	0.27	..	..	0.07	<0.02	..	..	..
		9,449							
High sensitivity Troponin I (ng/L)	<47	(9:57 am) 16,862	14,810	..	3212	339	151	61	39
		(2:16 pm)							
Creatine kinase (mU/mL)	24.0 – 190.0	671.0	509.0	..	..	49.0	..	..	45.0
White-cell count (per $\mu$ L)	4000 – 10,000	12,7500	7500	..	5380	5400	6540	6700	6440
Red-cell count (per $\mu$ L)	4300 – 5700	7170	6980	..	6850	6800	7100	7480	7090
Absolute neutrophil count (per $\mu$ L)	2000 – 8000	10,040	4000	..	3210	3900	3780	3880	3660
Absolute lymphocyte count (per $\mu$ L)	1500 – 4000	780	1900	..	1460	1000	1980	1920	1990
Platelet count (per $\mu$ L)	150,000 – 450,000	122,000	114,000	..	145,000	145,000	162,000	187,000	173,000
Haemoglobin (g/dL)	13.2 – 17.3	14.5	14.2	..	13.9	13.8	14.7	15.4	14.5
Haematocrit (%)	39.0 – 49.0	44.8	43.7	..	43.4	42.5	44.6	47.4	44.4
Mean Corpuscular Volume (fL)	82.0 – 98.0	62.4	62.6	..	63.3	62.5	62.9	63.4	62.6
Mean haemoglobin concentration (pg)	27.0 – 32.0	20.2	20.4	..	20.3	20.3	20.7	20.6	20.5



<b>Test</b>	<b>Specimen</b>	<b>Normal value</b>	<b>Result</b>
Adenovirus DNA (copies/mL)	Nasopharyngeal swab	<45	Undetectable
Parainfluenza 1 virus RNA (copies/mL)	Nasopharyngeal swab	<45	Negative
Parainfluenza 2 virus RNA (copies/mL)	Nasopharyngeal swab	<45	Undetectable
Chlamydomphila pneumoniae DNA	Nasopharyngeal swab	..	Negative
Mycoplasma pneumoniae DNA	Nasopharyngeal swab	..	Negative
Bordetella Pertussis DNA	Nasopharyngeal swab	..	Negative
Influenza A virus RNA (copies/mL)	Nasopharyngeal swab	<45	Undetectable
H1N1 Influenza A virus RNA	Nasopharyngeal swab	..	Negative
H2N2 Influenza A virus RNA	Nasopharyngeal swab	..	Negative
Influenza B virus RNA (copies/mL)	Nasopharyngeal swab	<45	Undetectable
Parainfluenza 3 virus RNA	Nasopharyngeal swab	..	Negative
Parainfluenza 4 virus RNA (copies/mL)	Nasopharyngeal swab	<45	Undetectable
Metapneumovirus RNA (copies/mL)	Nasopharyngeal swab	<45	Undetectable
Coronavirus OC43 RNA (copies/mL)	Nasopharyngeal swab	<50	0
Coronavirus 229E RNA (copies/mL)	Nasopharyngeal swab	<50	0
Coronavirus NL63 RNA (copies/mL)	Nasopharyngeal swab	<50	0
Coronavirus HKU RNA (copies/mL)	Nasopharyngeal swab	<50	0
Rhinovirus – Enterovirus RNA (copies/mL)	Nasopharyngeal swab	<45	Undetectable
Respiratory syncytial virus RNA (copies/mL)	Nasopharyngeal swab	<45	Undetectable
2019 Novel Coronavirus rRT-PCR	Nasopharyngeal swab	..	Positive
Enterovirus RNA (copies/mL)	Plasma	..	Undetectable
Hepatitis B surface antigen	Serum	..	Negative
Hepatitis C virus antibodies	Serum	..	Negative
HIV1-2 antibodies	Serum	..	Negative
HIV1 p24 antigen	Serum	..	Negative

rRT-PCR: Real-Time Reverse-Transcriptase–Polymerase-Chain-Reaction

**Table S3. Autoimmunity laboratory results**

<b>Test</b>	<b>Normal value</b>	<b>Result</b>
Lupus like anticoagulant aPTT (seconds)	26.00–36.00	33.30
Anti-Thyroglobulin antibody (IU/mL)	<40	<20
Anti-Thyreoperoxidase antibody (IU/mL)	<40	38.8
Anti-ENA (screening)	..	Negative
Anti-SCL70 (screening)	..	Negative
Anti-double-stranded-DNA (IU/mL)	<10	1.4
Anti-Cardiolipin IgM (IU/mL)	<10	3.0
Anti-Cardiolipin IgG (IU/mL)	<10	3.0
Anti-Mitochondrial antibody	<1:40	Negative
Anti-Nuclear antibody	..	Negative
Anti-Smooth-Muscle antibody	<1:40	Negative
Anti-Mitochondrial M2 antibody	..	Negative

## Methods

### *Specimen collection and diagnostic testing for SARS-CoV-2*

The treating physicians were responsible for the patient's data management and data protection with the aim of improving treatment and safety. Clinical specimens for SARS-CoV-2 testing were collected by using a sterile flexible nasopharyngeal nylon flocked premoistened swab (FLOQSwabs™, Copan Italia, Brescia, Italy) dipped in three mL universal transport medium (UTM™, Copan Italia, Brescia, Italy). Total nucleic acids (DNA/RNA) were extracted from 200 µL of UTM™ using the QIAsymphony® instrument with QIAsymphony® DSP Virus/Pathogen Midi Kit (Complex 400 protocol) according to the manufacturer's instructions (QIAGEN, Qiagen, Hilden, Germany). Specific real-time reverse transcriptase–polymerase chain reaction targeting RNA-dependent RNA polymerase and E genes were used to detect the presence of SARS-CoV-2 according to WHO guidelines<sup>1</sup> and Corman et al. protocols<sup>2</sup>.

### *Cardiac magnetic resonance*

Late Gadolinium Enhancement (LGE) Cardiac Magnetic Resonance (CMR) images were obtained using a 1.5T scanner (Magnetom Aera, Siemens Medical System, Erlangen, Germany) with a phased array cardiac coil and electrocardiogram gating.

Cine magnetic resonance images were acquired in two-chamber, four-chamber and three-chamber planes, then in short-axis with contiguous eight mm thick slices, from valve plane to ventricular apex, to assess ventricular function and cardiac kinesis. Both T2-weighted short-tau inversion recovery (T2w-STIR) and T2 mapping images were performed to assess myocardial oedema using the same planes.

Then, 0.1 mmol/kg of Gadolinium-DTPA (Gadovist; Bayer Schering Pharma, Berlin, Germany) was then administered and after ten minutes LGE images were obtained with a breath-hold 2-D segmented phase sensitive IR sequence, setting the acquisition window to mid-end diastole and using an inversion time between 240 and 300 milliseconds to null normal myocardium signal.

All CMR images were analysed using the CMR2 software (Circle Cardiovascular Imaging, Calgary, Alberta, Canada), manually drawing both endocardial and epicardial borders in the end-diastolic and end-systolic short-axis cine-steady-state free precession (SSFP) images. T2w-STIR images were visually assessed and all segments with signal intensity exceeding two standard deviations compared to normal myocardium were considered positive for oedema. The T2 mapping values of segments positive on T2w-STIR were obtained and compared to non-oedematous segments. LGE was considered present in areas with signal intensity exceeding five standard deviation compared to normal myocardium signal.

### **Discussion of the clinical case**

The number of patients impacted by the ongoing coronavirus disease 2019 (COVID-19) pandemic, caused by severe acute respiratory syndrome coronavirus 2 (SARS-CoV-2), continues to increase on a daily basis<sup>3-7</sup>. The majority of COVID-19 cases have mild symptoms and benign prognosis, but some evolve to severe clinical cases that can frequently be fatal. Although COVID-19 mainly affects the respiratory system, cardiac damage documented by elevation in cardiac troponin occurs in up to 28% of hospitalized COVID-19 adults and is negatively associated with mortality<sup>8,9</sup>. Surprisingly, cardiac involvement has also been described in a consistent percentage of paediatric patients, an observation that has important diagnostic and therapeutic implications<sup>10</sup>. While type 1 and 2 myocardial infarctions are expected to represent the most frequent causes of troponin elevation in adult patients, acute myocarditis is probably the leading cause of cardiac damage in the youngest patients, although so far there are no reported cases on this matter. It is known that viral infections are the most frequent cause of acute myocarditis<sup>11,12</sup> and other betacoronaviruses have already been associated with myocarditis<sup>13</sup>. A few cases of documented acute myocarditis in an adult COVID patient have also been

recently reported<sup>14,15</sup>. Here, we describe the first documented case of acute myocarditis as an isolated clinical manifestation in a paediatric patient positive for SARS-CoV-2 infection.

The mechanism through which this virus may cause myocardial damage is still unknown. It has been shown that SARS-CoV-2 infection of a variety of cell lines, including lung, bronchus, kidney, liver and colon cells, depends on the metalloproteinase Angiotensin-Converting Enzyme 2 (ACE2)<sup>16</sup>, that is highly expressed in the heart<sup>13</sup>. It therefore seems reasonable to suppose that SARS-CoV-2 may infect cardiomyocytes through ACE2 interaction and directly lead to cell death. It is also possible that cardiac damage is caused by an autoimmune reaction to self-antigens previously hidden to the immune system<sup>11,17</sup>. More studies are needed to unravel the prevalence and the pathophysiology of myocarditis in COVID-19 patients.

### **Acknowledgments**

We thank all the healthcare professionals involved in the management of the epidemic, the members of the COVID-19 IRCCS San Matteo Pavia Task Force, the patient and his family. The authors are grateful to Vanessa Marchesi, PhD, and Vanessa Cuccu, MS, for expert editorial support.

## References

- 1 World Health Organization. Diagnostic detection of 2019-nCoV by real-time RT-PCR. <https://www.who.int/docs/default-source/coronaviruse/protocol-v2-1.pdf>.
- 2 Corman VM, Landt O, Kaiser M, *et al.* Detection of 2019 novel coronavirus (2019-nCoV) by real-time RT-PCR. *Eurosurveillance* 2020; **25**: 2000045.
- 3 Zhu N, Zhang D, Wang W, *et al.* A Novel Coronavirus from Patients with Pneumonia in China, 2019. *N Engl J Med* 2020; **382**: 727–33.
- 4 Huang C, Wang Y, Li X, *et al.* Clinical features of patients infected with 2019 novel coronavirus in Wuhan, China. *Lancet* 2020; **395**: 497–506.
- 5 Wang D, Hu B, Hu C, *et al.* Clinical Characteristics of 138 Hospitalized Patients With 2019 Novel Coronavirus–Infected Pneumonia in Wuhan, China. *JAMA* 2020; **323**: 1061.
- 6 Yang X, Yu Y, Xu J, *et al.* Clinical course and outcomes of critically ill patients with SARS-CoV-2 pneumonia in Wuhan, China: a single-centered, retrospective, observational study. *Lancet Respir Med* 2020; published online Feb. DOI:10.1016/S2213-2600(20)30079-5.
- 7 Guan W-J, Ni Z-Y, Hu Y, *et al.* Clinical Characteristics of Coronavirus Disease 2019 in China. *N Engl J Med* 2020; published online Feb 28. DOI:10.1056/NEJMoa2002032.
- 8 Shi S, Qin M, Shen B, *et al.* Association of Cardiac Injury With Mortality in Hospitalized Patients With COVID-19 in Wuhan, China. *JAMA Cardiol* 2020; : 1–8.
- 9 Clerkin KJ, Fried JA, Raikhelkar J, *et al.* Coronavirus Disease 2019 (COVID-19) and Cardiovascular Disease. *Circulation* 2020; published online March 21. DOI:10.1161/CIRCULATIONAHA.120.046941.
- 10 Qiu H, Wu J, Hong L, Luo Y, Song Q, Chen D. Clinical and epidemiological features of 36 children with coronavirus disease 2019 (COVID-19) in Zhejiang, China: an observational cohort study. *Lancet Infect Dis* 2020; published online March. DOI:10.1016/S1473-3099(20)30198-5.
- 11 Caforio ALP, Pankuweit S, Arbustini E, *et al.* Current state of knowledge on aetiology, diagnosis, management, and therapy of myocarditis: a position statement of the European Society of Cardiology Working Group on Myocardial and Pericardial Diseases. *Eur Heart J* 2013; **34**: 2636–48.
- 12 Kindermann I, Barth C, Mahfoud F, *et al.* Update on Myocarditis. *J Am Coll Cardiol* 2012; **59**: 779–92.
- 13 Hendren NS, Drazner MH, Bozkurt B, Cooper, Jr. LT. Description and Proposed Management of the Acute COVID-19 Cardiovascular Syndrome. *Circulation* 2020; published online April 16. <https://doi.org/10.1161/CIRCULATIONAHA.120.047349>.
- 14 Inciardi RM, Lupi L, Zacccone G, *et al.* Cardiac Involvement in a Patient With Coronavirus Disease 2019 (COVID-19). *JAMA Cardiol* 2020; published online March 27. DOI:10.1001/jamacardio.2020.1096.
- 15 Doyen D, Mocerri P, Ducreux D, Dellamonica J. Myocarditis in a patient with COVID-19: a cause of raised troponin and ECG changes. *Lancet* 2020; **395**: 1516.
- 16 Hoffmann M, Kleine-Weber H, Schroeder S, *et al.* SARS-CoV-2 Cell Entry Depends on ACE2 and TMPRSS2 and Is Blocked by a Clinically Proven Protease Inhibitor. *Cell* 2020; **181**: 271–80.
- 17 Fung G, Luo H, Qiu Y, Yang D, McManus B. Myocarditis. *Circ Res* 2016; **118**: 496–514.